

Green Chemistry

Accepted Manuscript



This is an *Accepted Manuscript*, which has been through the Royal Society of Chemistry peer review process and has been accepted for publication.

Accepted Manuscripts are published online shortly after acceptance, before technical editing, formatting and proof reading. Using this free service, authors can make their results available to the community, in citable form, before we publish the edited article. We will replace this *Accepted Manuscript* with the edited and formatted *Advance Article* as soon as it is available.

You can find more information about *Accepted Manuscripts* in the [Information for Authors](#).

Please note that technical editing may introduce minor changes to the text and/or graphics, which may alter content. The journal's standard [Terms & Conditions](#) and the [Ethical guidelines](#) still apply. In no event shall the Royal Society of Chemistry be held responsible for any errors or omissions in this *Accepted Manuscript* or any consequences arising from the use of any information it contains.



www.rsc.org/greenchem

Efficient biomass transformations catalyzed by graphene-like nanoporous carbons functionalized with strong acid ionic liquids and sulfonic group

Fujian Liu ^{a,c}, Weiping Kong ^a, Liang Wang ^c, Xianfeng Yi ^b, Iman Noshadi ^d, Anmin Zheng*^b and Chenze Qi*^a

^a Key Laboratory of Alternative Technologies for Fine Chemicals Process of Zhejiang Province, Department of Chemistry, Shaoxing University, Shaoxing, 312000, China.

E-mail: qichenze@usx.edu.cn

^b Wuhan Center for Magnetic Resonance, State Key Laboratory of Magnetic Resonance and Atomic and Molecular Physics, Wuhan Institute of Physics and Mathematics, Chinese Academy of Sciences, Wuhan 430071, China.

E-mail: zhenganm@wipm.ac.cn

^c Department of Chemistry, Zhejiang University (XiXi Campus), Hangzhou, 310028, China.

^d Polymer Program, Institute of Materials Science and Department of Chemistry, University of Connecticut, Storrs, CT, 06269, United States.

Abstract

Strong acid ionic liquids and sulfonic group bifunctional graphene-like nanoporous carbons (GNC-SO₃H-ILs) have been synthesized from treating nitrogen

containing graphene-like nanoporous carbons (GNCs) with 1,3-propanesultone, ion exchanging with HSO_3CF_3 or H_2SO_4 . Introducing nitrogen is important for grafting strong acid ionic liquids and sulfonic group in GNCs, which were synthesized from carbonization of a mixture of dicyandiamide or melamine and glucose. GNC-SO₃H-ILs possess abundant nanopores, nanosheet structure, good dispersion and controlled acidity. By themselves, they are capable of enhancing the fast diffusion of reactants and products, while increasing the exposition degree of acidic sites in GNC-SO₃H-ILs throughout various reactions. The above characters result in their much improved catalytic activity in biomass transformation such as production biodiesel and depolymerization of crystalline cellulose into sugars, which were even as comparable as those of homogeneous ionic liquid and mineral acids.

Keywords: Graphene-like nanoporous carbons, biomass transformation, nanosheet, solid acids, accessibility.

1. Introduction

Great effort has been made to develop efficient and cost effective ways to transform biomass into biofuels, due to its low cost, excellent renewability and environmental friendliness when compared with conventional fossil energy¹⁻⁹. Biomass may therefore be the most important feedstock for replacing conventional fossil energy in the future. Generally, biofuels were typically produced from two routes: (i) towards transesterification to biodiesel and (ii) depolymerization of

crystalline cellulose into sugars and fine chemicals ^{1, 2, 7, 10-15}. Notably, biodiesel production was focused on employing low cost and low quality plant oil or waste oil as the feedstocks, typically held under green and mild conditions ¹⁶. Alternatively, the depolymerization of cellulose was mostly held under severe conditions ^{7, 9}. Surprisingly, crystalline cellulose easily transformed into sugars in the presence of alkylmethylimidazolium ionic liquids solvents because of their unique ability to break down the crystalline cellulose into soluble polymer chains. However, the high cost of ionic liquids and the reaction mixtures acute recyclability creates a demand for new catalysts, with extremely high effectiveness. Researchers have discovered that acids, bases or enzyme catalysts were active when producing biomass transformations ^{1, 2, 7, 10-16}. Acid catalysts were highly efficient and low in cost for biomass transformation, which could catalyze transformation of low-quality and low cost biomass into biofuels under rather mild conditions. The replacement of mineral acids with solid acids in terms of biomass transformation has received considerable attention regarding green and sustainable chemistry ¹⁰⁻¹⁹.

Among various heterogeneous acid catalysts, carbon based solid acids showed controlled wettability, good thermal and chemical stabilities and superior catalytic activity throughout various reactions, combining the advantages of the solid acids with both organic and inorganic frameworks ^{3, 20-24}. Graphene based nanomaterials act as novel carbon materials. Materials scientists, chemists and physicist recognize these materials to possess excellent thermal and mechanical stabilities, unique nanosheet structure, controlled wettability and very good dispersion in various systems ²⁵⁻³⁰.

These are the ideal candidates for solid acidic catalysts or catalyst supports because they are capable of largely reducing the limitation of mass transfer, increase the exposition degree of active sites and enhance the recyclability of the catalysts in various reactions³¹⁻³³. Do to the frequency of graphene nanomaterial layers sticking together, it is imperative to create pillars between the layers, maximizing the surface area and accessibility during various reactions³¹⁻³³. Still, synthesis of graphene based nanomaterials with large BET surface areas and abundant nanopores through facile and cost-effective routes remains a challenge³⁴⁻³⁸. Abundant nanopores in graphene-based nanomaterials must be created to increase the degree of active sites, which contribute importantly to their application during heterogeneous catalysis³¹.

We report here the successful synthesis of novel acid ionic liquids and sulfonic group bifunctional graphene-like nanoporous carbons (GNC-SO₃H-ILs), which were synthesized by treating nitrogen containing graphene-like nanoporous carbons (GNCs) with 1,3-propanesultone. The anions were exchanged with strong acids of H₂SO₄ or HSO₃CF₃. The introduction of nitrogen atom in GNCs forms strong acid ionic liquids and sulfonic group through the quaternary ammonization reaction. The GNCs supports could be easily synthesized using a one-step carbonization mixture. This mixture should consist of dicyandiamide/melamine and glucose, using no additional templates (As shown in Scheme 1). The resultant bifunctional carbon based solid acids showed controlled acidity, unique nanosheet structure, abundant nanopores and good stability. Interestingly, GNC-SO₃H-ILs significantly improved catalytic activity and good recyclability in biomass transformation, including transesterification to

biodiesel and depolymerization of crystalline cellulose into sugars and 5-hydroxymethylfurfural (HMF). This process was better than those of acidic resin of Amberlyst 15, sulfonic group functionalized mesoporous SBA-15, and heteropolyacid of $\text{H}_3\text{PW}_{12}\text{O}_{40}$, which was even as comparable as those of homogeneous acid ionic liquids and mineral acids. The preparation of GNC-SO₃H-ILs fosters a facile and cost-effective method to synthesize highly efficient graphene based solid acids for biomass transformation, which is crucial for their various applications when exploring biofuel through green and sustainable processes.

2. Experimental details

2.1 Preparation of catalysts

2.1.1 Synthesis of GNCs

GNCs were synthesized from carbonization of the mixture of melamine and glucose with various weight ratios under N₂ condition. Typically, 0.1 g of glucose and 4.0 g of melamine were mixed together. After grinding of the mixture for 10 minutes, the sample was transferred into the tube furnace under flowing N₂ condition. The temperature of tube furnace experienced the following heating processes: from room temperature to 600 °C (2.5 °C/min), from 600 °C to 800 °C (1.67 °C/min), and remained at 800 °C for 1 h. After cooling the furnace to room temperature, GNCs with monolithic morphology were obtained. Moreover, GNCs could also be synthesized from the carbonization of the mixture of dicyandiamide and glucose using similar

weight ratios, under similar conditions.

2.1.2 Synthesis of strong acid ionic liquids and sulfonic group bifunctional GNCs (GNC-SO₃H-ILs).

GNC-SO₃H-ILs were synthesized from quaternary ammonization of GNCs with 1,3-propanesultone, and anion exchange with strong acids of H₂SO₄ or HSO₃CF₃. As a typical run for synthesis of GNC-[C₃N][SO₃CF₃], 1.2 g of GNC were added into a mixture containing 20 mL of toluene and 0.3 g of 1,3-propanesultone. After heating the reaction mixture at 110 °C for 24 h under refluxing, the reaction mixture was cooled down to room temperature (25 °C). The sample was then treated with a solution containing 25 mL of toluene and 3-5 mL HSO₃CF₃ for 24 h at room temperature upon vigorous stirring. GNC-[C₃N][SO₃CF₃] could be obtained from filtering, washing with a large amount of CH₂Cl₂ to remove the residual HSO₃CF₃, and then drying it at 60 °C for 12 h. This procedure was repeated twice. GNC-[C₃N][SO₃CF₃] was then obtained, where [SO₃CF₃] stands for the treating acid of trifluoromethanesulfonic acid and C₃ stands for 1,3-propanesultone. The detailed synthetic procedures of GNC-[C₃N][SO₃CF₃] was also shown in Scheme 1. For comparison, [C₃vim][SO₃CF₃] ("C₃" stands for 1,3-propanesultone, "vim" stands for vinyl imidazole and "[SO₃CF₃]" stands for the treating acid of HSO₃CF₃) and SBA-15-SO₃H (S/Si=0.2, "SBA" stands for ordered mesoporous silicas) was synthesized according to the literature^{8,39},

2.2 Catalytic reactions

2.2.1 Transesterification

Transesterification of tripalmitin with methanol was executed as follows: 0.84 g (1.04 mmol) of tripalmitin was melted into a flask equipped with a condenser and magnetic stirrer at 65 °C. Then, 0.10 g of catalyst was quickly added upon vigorous stirring to form a homogeneous mixture. An additional 2.47 mL (61 mmol) of methanol was added, after further stirring of the mixture for 14 h at 65 °C under refluxing, the reaction was finished; the catalysts could be separated by centrifugation. The molar ratio of tripalmitin/methanol was 1/60 and the mass ratio of catalyst/tripalmitin was 0.119. The product was methyl palmitate with selectivity near 100 %, which was analyzed by gas chromatography of Agilent 7890 with a flame ionization detector (FID). The column was HP-INNOWax capillary column (30 m); the initial temperature was 100 °C, ramping rate was 20 °C/min, and the final temperature was 280 °C; the temperature of FID detector was 350 °C. In this reaction, the concentration of methyl palmitate was calculated through the internal standard (dodecane) method, establishing the standard curve.

Transesterification of sunflower oil with methanol was executed as follows: 1.0 g of sunflower oil (1.16 mmol) was added into a flask equipped with a condenser and magnetic stirrer. The temperature was rapidly increased to 65 °C. Then, 3.5 mL of methanol (86.3 mmol) and 0.15 g of catalyst were quickly upon under vigorous stirring. The reaction was occurred for 18 h. The molar ratio of sunflower oil to methanol was 1/75 and the mass ratio of catalyst to tripalmitin was 0.1. The products were mainly methyl palmitate (C_{16:0}), methyl stearate (C_{18:0}), methyl oleate (C_{18:1}),

methyl linoleate (C_{18:2}), and methyl heptacosane (C_{27:0}). The quantification of these products were analyzed by using Agilent GC/MS instrument (Agilent 6890N/5975I) with a programmable split/splitless injector.

2.2.2 Catalysts regeneration

1.0 g (1.04 mmol) of sunflower oil was melted into a flask equipped with a condenser and magnetic stirrer at 65 °C. Then, 0.15 g of catalyst was quickly added upon vigorous stirring to form a homogeneous mixture, then by an addition of 2.47 mL (61 mmol) of methanol, after having stirred the mixture for 18 h at 65 °C under reflux. Centrifugation was then carried out for catalyst separation. The catalyst was used for the next run after washing the sample with a large amount of CH₂Cl₂, which removed the absorbed reactants and products and drying it under a vacuum condition.

2.2.3 Depolymerization of crystalline cellulose into sugars and HMF

The depolymerization of crystalline cellulose from Avicel was also chosen as the model reaction for evaluating the activities of various catalysts. As a typical run for depolymerization of Avicel, 100 mg of crystalline cellulose of Avicel was dissolved into a mixture containing 1.5 g of [C₄mim]Cl ionic liquid and 0.5 mL of DMSO at 100 °C for 3-5 h upon vigorous stirring until a clear solution was obtained, followed an additional 20 mg of GNC-[C₃N][SO₃CF₃]. Then, 600 μL of water was slowly introduced into the reaction mixture while the reaction temperature was remained at 100 °C. At different time intervals, samples were withdrawn, weighed, quenched

immediately with cold water, and centrifuged at 14,800 rpm for 5 min to remove catalysts and unreacted cellulose, giving the reaction mixture. Various acid catalysts such as Amberlyst 15, HCl and $[\text{C}_3\text{vim}][\text{SO}_3\text{CF}_3]$ were also used for catalyzing depolymerization of Avicel, which were used the same number of acidic sites as in GNC- $[\text{C}_3\text{N}][\text{SO}_3\text{CF}_3]$.

Meanwhile, the isolated cellulose was thoroughly washed with water, and recovered through centrifugation. The amount of cellulose isolated was determined by weight.

Testing Total Reducing Sugar (TRS)

TRS value was usually used for evaluating the depolymerization degree of crystalline cellulose catalyzed by various catalysts, which was tested through DNS method ^{7, 9, 14}. As a typical run, a mixture containing of 0.5 mL of 3,5-dinitrosalicylic acid (DNS) reagent and 0.5 mL of performed reaction mixture was heated for 5 min at 100 °C, then cooled to room temperature. Then, 4 mL of deionized water was added to dilute the mixture. The color intensity of the mixture was measured in a NanoDrop 2000 UV-spectrophotometer at 540 nm. The concentration of the total reducing sugars was calculated based on a standard curve obtained with glucose.

The concentrations of glucose and cellobiose in the reaction mixture were measured by the Shimadzu LC-20A HPLC system based on standard curve method, which was equipped with a SCR-101N column using extra-pure water during mobile phase at a flow rate of 0.5 mL/min. The column's temperature was set to 55 °C. In the

meantime, a refraction index was used for detection sugars in the water; The concentration of 5-hydroxymethylfurfural (HMF) was also measured by Shimadzu LC-20A HPLC system, based on standard curve method. It was equipped with a CAPCELL PAK C18 column using methanol and water (methanol/water=80:20) during the mobile phase, at a flow rate of 0.7 mL/min and the column's temperature was set to 50 °C. At the same time, an ultraviolet detector with the wavelength number at 254 nm was used for detection HMF in the reaction mixture.

3. Results and discussion

3.1 Structural characterizations

Figure 1A showed XRD patterns of GNC and GNC-[C₃N][SO₃CF₃]. Notably, GNC exhibits two broad peaks centered at 26.1 and 43.2 °. These are associated with the graphite structure, which was extremely close to the peaks of graphene based nanomaterials with a nanosheet structure, reported previously^{31,37}. It is indicated the formation of apparently graphene-like structures with several layers in the GNC support. After grafting the strong acid ionic liquids and the sulfonic group onto the network of GNC, the sample of GNC-[C₃N][SO₃CF₃] was given, which showed almost no change in XRD patterns compared to the GNC support. The above results indicated the graphene-like nanosheet structure was well maintained in GNC-[C₃N][SO₃CF₃].

In addition, the graphene-like structures of GNC and GNC-[C₃N][SO₃CF₃] have also been confirmed by the Raman spectra. It is well known that Raman spectroscopy

is a powerful approach to determining the properties of graphene based nanomaterials such as the number and orientation of layers, the quality and types of edges and the effects of perturbations involving the structure strain, doping, disorder and functional groups^{40,41}. Figure 1B showed the Raman spectra of GNC and GNC-[C₃N][SO₃CF₃]. It was noted that a series of peaks at approximately 1378, 1591, 2639 and 2822 cm⁻¹ were clearly observed in these samples, which could be attributed to the signals of D, G, 2D and S3 bands²⁶. The broaden D-band indicated the presence of sp³ carbon atoms with defects and disorders at the edges and the boundaries of the graphene domains. The sharp G-band indicated the presence of sp² carbon atoms in a graphitic 2D hexagonal lattice, confirming the formation of graphitic carbon, in good agreement with XRD results. Compared with GNC, GNC-[C₃N][SO₃CF₃] showed a decreased intensity of Raman spectrum, which could be attributed to the introduction of acidic groups in the sample. It is also noteworthy that the position and shape of each peak in the Raman spectrum dose not shift after the introduction of acidic groups in GNC. This indicates that the graphene-like nanosheet structure was well maintained in GNC-[C₃N][SO₃CF₃], in good agreement with XRD results.

Table 1 presented the parameters of various acid catalysts. GNC-[C₃N][SO₃CF₃] showed the content of acidic sites at 1.25 mmol/g, lower than those of various acid catalysts including SBA-15-SO₃H (1.98 mmol/g), H₃PW₁₂O₄₀ (3.5 mmol/g), Amberlyst 15 (4.3 mmol/g) and H₂SO₄ (10.2 mmol/g). Alternatively, the BET surface area of GNC-[C₃N][SO₃CF₃] (184 m²/g, Figure S1) was higher than that of acidic resin of Amberlyst 15 (45 m²/g). Compared to GNC support (945 m²/g), the decreased

surface area in GNC-[C₃N][SO₃CF₃] should result from the grafting of acid active sites, which largely increases the weight of the GNC network. Previously, similar results have also been reported ³⁹.

In order to obtain the relationship between the catalyst structure and reactive activity, the surface morphology of the GNC-[C₃N][SO₃CF₃] was analyzed in detailed by the multiple image techniques (TEM, HR-TEM and AFM images). Typically, TEM images indicate typically nanosheet structure with three dimensional network clusters in GNC-[C₃N][SO₃CF₃], exhibiting abundant nanoporous and hollow structures (Figure 2a&b, Figure S2). Furthermore, high-resolved TEM images were also used to confirm the graphene structure with crumpled and entangled characters (Figure 2c-f, Figure S1), exhibiting several nanocrystallites with well-defined lattice planes. When the XRD and Raman as aforementioned were combined with TEM and HR-TEM, the uniform graphitized networks were determined. In the meantime, the AFM image of GNC-[C₃N][SO₃CF₃] further affirms it's nanosheet structure (Figure 2g). The thickness of layers were ranged from 1.7 to 3.5 nm, indicating the stick had several graphene layers in GNC-[C₃N][SO₃CF₃]. These results confirmed the graphene-like nanoporous carbon network was formed in GNC-[C₃N][SO₃CF₃].

Figure 3 showed the X-ray photoelectron spectroscopy (XPS) spectra of GNC-[C₃N][SO₃CF₃], which exhibits the signals of S_{2p} (168.8 eV), C_{1s} (284.8 eV), N_{1s} (402.1 eV), O_{1s} (532.4 eV) and F_{1s} (686.8 eV). Notably, the broad C_{1s} spectrum could be fitted and deconvoluted into four peaks, centered at approximately 284.8, 286.1, 287.0 and 292.3 eV, which should be assigned to C-C and C-N in GNC

network, and C-O and C-F in the strongly acidic ionic liquids and sulfonic group⁸. In the meantime, the N_{1s} spectrum could be fitted and deconvoluted into two peaks, centered at approximately 398.4, 400.4 and 401.8 eV, which should be assigned to C-N, N⁺-C₃ ionic liquid group and protonated structure of GNC-[N⁺H][SO₃CF₃] in GNC-[C₃N][SO₃CF₃]⁸. Similarly, the O_{1s} associated with O-S (531.9 eV) and O-SCF₃ (533.1 eV) could also be observed⁸. The above results confirm that strongly acidic ionic liquids and sulfonic group have been successfully grafted onto the network of GNCs, in good agreement with FT-IR and elemental analysis results (Figure S3 & Table 1).

Furthermore, the acidity properties of GNC-[C₃N][SO₃CF₃] were also characterized by the ³¹P NMR probe techniques involving the adsorbed trimethylphosphine (TMP) and trimethylphosphine oxygen (TMPO). It is noteworthy that the ³¹P NMR probe technique is a sensitive and reliable technique to determine the acid type (Brønsted or Lewis acid) and acid strength of solid acid catalysts⁴²⁻⁴⁴. As shown in Figure 4a, using TMP as a probe molecule, the ³¹P resonances at -3.2 ppm was assigned to the protonated adducts of [(CH₃)₃P-H]⁺, and attributed to the reaction of TMP with the Brønsted acidic protons. On the contrary, almost no resonances were observed in the range of -20 to -60 ppm due to the interaction with Lewis acid sites^{42, 43}. Therefore, it is indicative that no Lewis acid was formed over GNC-[C₃N][SO₃CF₃]. As aforementioned introduction, solid-state ³¹P MAS NMR of adsorbed TMPO is an efficient technique for acidity characterization of solid acid catalysts such as zeolites, sulfated mesoporous metal oxides and heteropolyacids^{42, 43}.

Interestingly, GNC-[C₃N][SO₃CF₃] showed multiple ³¹P resonance peaks at approximately 45, 48, 51.2, 52.8, 54.5, 56.6 and 63.1 ppm, indicating presence of various Brønsted acid sites with different acid strengths in GNC-[C₃N][SO₃CF₃] (Figure 4b). The weak acidic sites (45&48 ppm) may be attributed to presence of the carboxylic or hydroxyl group in GNC-[C₃N][SO₃CF₃]; While the relative strongly acidic sites (51.2, 52.8, 54.5, 56.6 and 63.1 ppm) should be attributed to strong acid ionic liquids, sulfonic group and protonated structure of GNC-[N⁺H][SO₃CF₃] located in outer and inner surfaces of GNC-[C₃N][SO₃CF₃]. The GNC-[N⁺H][SO₃CF₃] structure should be formed from protonation of the N atom in GNC by HSO₃CF₃. It's noteworthy that the acidity of the -SO₃H group is stronger than GNC-[N⁺H][SO₃CF₃], and -SO₃H group has a better catalytic roles for its activity. The strong acidic sites in GNC-[C₃N][SO₃CF₃] showed similar acid strength with that of HY zeolites (55 and 65 ppm) and bifunctional carbon-silica nano composited solid acid (40-70 ppm)^{44,45}.

3.2 Catalytic reactions

3.2.1 Towards transesterification to biodiesel

Figure 5 showed the dependences of catalytic activities on the time in transesterification of tripalmitin with methanol catalyzed by various samples. Notably, GNC-[C₃N][SO₃CF₃] showed much better catalytic activity than those of H₃PW₁₂O₄₀, SBA-15-SO₃H and Amberlyst 15. For instance, the yield of biodiesel (methyl palmitate) catalyzed by GNC-[C₃N][SO₃CF₃] was up to 78.8 % after 10 h of reaction, much higher than those of H₃PW₁₂O₄₀ (51.6 %), SBA-15-SO₃H (50.5 %) and

Amberlyst 15 (39.7 %); Increasing the reaction time up to 14 h, the yield of methyl palmitate catalyzed by GNC-[C₃N][SO₃CF₃] was increased up to 88.5 %. This was even as comparable to that of the homogeneous acid ionic liquid of [C₃vim][SO₃CF₃] (89.8 %). On the contrary, H₃PW₁₂O₄₀, SBA-15-SO₃H and Amberlyst 15 still gave relatively lower biodiesel yields at 64.1, 60.8 and 53.6 %, respectively.

Except for tripalmitin, GNC-[C₃N][SO₃CF₃] also showed good catalytic activity for transformation of plants oils such as sunflower oil into biodiesel. Table 2 presented catalytic data in transesterification of sunflower oil with methanol for the production of biodiesel over various catalysts. Interestingly, after 18 h of reaction, the yields of biodiesel including C_{16:0}, C_{18:0}, C_{18:1}, C_{18:2} and C_{27:0} catalyzed by GNC-[C₃N][SO₃CF₃] were almost as high as inside the pure acidic ionic liquid of [C₃vim][SO₃CF₃] (89.1, 94.8, 95.2, 93.1, 86.7 % in homogeneous, Vs 88.5, 93.6, 94.7, 92.3 and 81.4 % in heterogeneous), which were even as comparable as that of H₂SO₄ (87.4, 94.1, 95.9, 94.4 and 82.1 %). Therefore, it is clear that the high catalytic reactivity has been well remained. As presented in Table 2, the activity of GNC-[C₃N][SO₃CF₃] was much higher than those of heteropolyacid of H₃PW₁₂O₄₀ (58.9, 59.2, 54.3, 60.1 and 50.9 %), Amberlyst 15 (54.8, 50.2, 48.6, 50.5 and 26.4 %) and SBA-15-SO₃H (60.9, 56.5, 55.4, 52.6 and 45.7 %). The excellent catalytic activity found in GNC-[C₃N][SO₃CF₃] for biodiesel production could be attributed to its controlled acidity, good dispersion, abundant and hierarchical nanoporosity, and unique nanosheet structure. By themselves, they are capable of enhancing the fast diffusion of reactants and products, increasing exposition degree of catalytically active sites, in processes of various

reactions. Compared to GNC-[C₃N][SO₃CF₃], the low BET surface areas of H₃PW₁₂O₄₀ and Amberlyst 15 resulted in their low exposition degrees and easy poison of active sites, further leading to their low catalytic activities. Although SBA-15-SO₃H has large BET surface areas, its functional group could be easily occluded in the silica wall⁴⁶; Moreover, the accessibility of reactants to catalytically active sites located into the mesopores of SBA-15-SO₃H are usually difficult in comparison to two dimensional nanosheet structures of GNC-[C₃N][SO₃CF₃]²⁷. These factors resulted in a lower catalytic activity of SBA-15-SO₃H. The above results prove that GNC-[C₃N][SO₃CF₃] could be used as highly efficient solid acid for biodiesel production.

More importantly, GNC-[C₃N][SO₃CF₃] showed very good recyclability for catalyzing biodiesel production. For example, in the reaction of sunflower oil with methanol, even after being recycled for five times, the yields of biodiesel catalyzed by GNC-[C₃N][SO₃CF₃] were still up to 86.2, 90.8, 92.1, 89.4 and 79.5 % (Table 2), comparable to fresh GNC-[C₃N][SO₃CF₃] (88.5, 93.6, 94.7, 92.3 and 81.4 %, Table 2).

3.2.2 Depolymerization of crystalline cellulose into biofuels

To further decrease the cost of biofuels, much effort has been made to develop green and cost-effective ways to produce renewable biofuels from cellulosic biomass, in recent years. The depolymerization of crystalline cellulose (Avicel) into sugars, catalyzed by various acid catalysts has also been investigated in this work, and was achieved in presence of 1-n-butyl-3-methylimidazolium and DMSO mixed solvents.

Figure 6 showed the dependences of catalytic activities on the time in depolymerization of Avicel catalyzed by GNC-[C₃N][SO₃CF₃], Amberlyst 15, HCl and [C₃vim][SO₃CF₃]. Notably, GNC-[C₃N][SO₃CF₃] showed significantly better catalytic activity than that of Amberlyst 15, one of the most efficient commercially acidic resins, comparable to those of homogeneous HCl and [C₃vim][SO₃CF₃] (the same number of active sites as in GNC-[C₃N][SO₃CF₃]). For example, the yields of total reducing sugars, mono- and disaccharides catalyzed by GNC-[C₃N][SO₃CF₃] was 94.6 % after 5 h of incubation, higher than those of Amberlyst 15 (40.5 %), HCl (87.1 %) and [C₃vim][SO₃CF₃] (84.9 %). Similar results could also be obtained from HPLC data (As shown in Table 3), the yields of the main products including glucose (44.1 %), cellobiose (32.7 %) and HMF (11.6 %) catalyzed by GNC-[C₃N][SO₃CF₃] were much higher than that of Amberlyst 15 (14.3, 17.5 and 3.2 %), which were as comparable as those of homogeneous HCl (39.8, 20.4 and 10.7 %) and [C₃vim][SO₃CF₃] (26.3, 34.5 and 10.1 %). Presumably, the drastic enhancement of the catalytic effectiveness found in GNC-[C₃N][SO₃CF₃] during biomass transformation was attributed to the synergistic effects from the abundant nanopores, unique nanosheet structure, good dispersion, controlled acidity and good network stability of the catalyst.

The preparation of GNC-[C₃N][SO₃CF₃] will open an effective method for synthesizing graphene-like nanoporous carbon based solid acids with excellent catalytic activity and a long life for biomass transformation, which will be potentially important for the wide applications of graphene based nanomaterials in the areas of

biofuel exploitation in the near future.

4. Conclusion

Efficient graphene-like nanoporous carbons based solid acids (GNC-SO₃H-ILs) were successfully synthesized and tested for their effectiveness in biomass transformation. GNC-SO₃H-ILs showed controlled acidity, abundant nanopores, unique nanosheet structure and good dispersion in various reaction media, resulting in their excellent catalytic efficiency for biodiesel production and depolymerization of crystalline cellulose into biofuel precursors. The preparation of GNC-SO₃H-ILs will offer a facile and cost-effective way to synthesize nanoporous graphene based solid strong acids, which will be very important for their wide applications in the areas of biofuel production through green and sustainable processes.

Acknowledgements

This work was supported by the National Natural Science Foundation of China (21203122 and 21173255), the Foundation of Science, Key Sci-Tech Innovation Team Project of Zhejiang Province (2010R50014-20), Postdoctoral Foundation of China (2012M520062, Bsh1201018), the Foundation of State Key Laboratory of Magnetic Resonance and Atomic and Molecular Physics, Wuhan Institute of Physics and Mathematics, Chinese Academy of Sciences (T151303) and State Key Laboratory of Inorganic Synthesis and Preparative Chemistry, Jilin University (2013-12).

References

- 1 G. W. Huber, S. Iborra and A. Corma, *Chem. Rev.* 2006, **106**, 4044.
- 2 A. Corma, S. Iborra and A. Velty, *Chem. Rev.* 2007, **107**, 2411.
- 3 M. Toda, A. Takagaki, M. Okamura, J. N. Kondo, S. Hayashi, K. Domen and M. Hara, *Nature* 2005, **438**, 178.
- 4 Y. Román-Leshkov, C. J. Barrett, Z. Y. Liu and J. Dumesic, *Nature* 2007, **447**, 982.
- 5 G. W. Huber, J. N. Chheda, C. J. Barrett and J. A. Dumesic, *Science*, 2005, **308**, 1446.
- 6 Y. Román-Leshkov, J. N. Chheda and J. A. Dumesic, *Science*, 2006, **312**, 1933.
- 7 R. Rinaldi and F. Schüth, *ChemSusChem*, 2009, **2**, 1096.
- 8 F. J. Liu, L. Wang, Q. Sun, L. F. Zhu, X. J. Meng and F.-S. Xiao, *J. Am. Chem. Soc.*, 2012, **134**, 16948.
- 9 F. J. Liu, R. K. Kamat, I. Noshadi, D. Peck, R. S. Parnas, A. Zheng, C. Qi and Y. Lin, *Chem. Comm.*, 2013, **49**, 8456.
- 10 J. B. Binder and R. T. Raines, *J. Am. Chem. Soc.*, 2009, **131**, 1979.
- 11 F. J. Liu, A. M. Zheng, I. Noshadi and F.-S. Xiao, *Appl. Catal., B*, 2013, **136-137**, 193.
- 12 J. B. Binder and R. T. Raines, *Proc. Natl. Acad. Sci. U. S. A.*, 2010, **107**, 4516.
- 13 L. Wang, H. Wang, F. J. Liu, A. Zheng, J. Zhang, Q. Sun, J. P. Lewis, L. Zhu, X. Meng and F.-S. Xiao *ChemSusChem*, 2014, **7**, 402.

- 14 R. Rinaldi, R. Palkovits and F. Schüth, *Angew. Chem., Int. Ed.*, 2008, **47**, 8047.
- 15 F. M. A. Geilen, B. Engendahl, A. Harwardt, W. Marquardt, J. Klankermayer and W. Leitner, *Angew. Chem., Int. Ed.*, 2010, **49**, 5510.
- 16 I. Noshadi, B. Kanjilal, S. C. Du, G. M. Bollas, S. L. Suib, A. Provasas, F. J. Liu and R. S. Parnas, *Applied Energy* 2014, **129**, 112.
- 17 A. Corma, *Chem. Rev.*, 1997, **97**, 2373.
- 18 F. Su and Y. H. Guo, *Green Chem.*, 2014, **16**, 2934.
- 19 H. L. Cai, C. Z. Li, A. Q. Wang, G. L. Xu and T. Zhang, *Appl. Catal., B*, 2012, **123-124**, 333.
- 20 S. Suganuma, K. Nakajima, M. Kitano, D. Yamaguchi, H. Kato, S. Hayashi and M. Hara, *J. Am. Chem. Soc.*, 2008, **130**, 12787.
- 21 M. Hara, T. Yoshida, A. Takagaki, T. Takata, J.N. Kondo, S. Hayashi and K. Domen, *Angew. Chem. Int. Ed.*, 2004, **43**, 2955.
- 22 R. Xing, Y. M. Liu, Y. Wang, L. Chen, H. H. Wu, Y. W. Jiang, M. Y. He and P. Wu, *Micro. Meso. Mater.*, 2007, **105**, 41.
- 23 Z. X. Ding, X. F. Chen, M. Antonietti and X. C. Wang, *ChemSusChem* 2011, **4**, 274.
- 24 Y. Zhang, A. Thomas, M. Antonietti and X. Wang, *J. Am. Chem. Soc.* 2009, **131**, 50.
- 25 K. S. Novoselov, A. K. Geim, S. V. Morozov, D. Jiang, Y. Zhang, S. V. Dubonos, I. V. Grigorieva and A. A. Firsov, *Science* 2004, **306**, 666.
- 26 A. K. Geim, *Science* 2009, **324**, 1530.

- 27 K. S. Noveselov, A. K. Geim, S. V. Morozov, D. Jiang, M. I. Katsnelson, I. V. Grigorieva, S. V. Dubonos and A. A. Firsov, *Nature* 2005, **438**, 197.
- 28 M. A. Worsley, P. J. Pauzauskie, T. Y. Olson, J. Biener, J. H. Satcher, Jr. and T. F. Baumann, *J. Am. Chem. Soc.*, 2010, **132**, 14067.
- 29 S. B. Yang, X. L. Feng, X. C. Wang and K. Müllen, *Angew. Chem. Int. Ed.*, 2011, **50**, 5339.
- 30 X.-H. Li, J.-S. Chen, X. C. Wang, M. E. Schuster, R. Schlögl and M. Antonietti, *ChemSusChem* 2012, **5**, 642.
- 31 F. J. Liu, J. Sun, L. F. Zhu, X. J. Meng, C. Z. Qi and F.-S. Xiao, *J. Mater. Chem.*, 2012, **22**, 5495.
- 32 P. P. Upare, J.-W. Yoon, M. Y. Kim, H.-Y. Kang, D. W. Hwang, Y. K. Hwang, H. H. Kung and J.-S. Chang, *Green Chem.*, 2013, **15**, 2935.
- 33 H. L. Wang, T. S. Deng, Y. X. Wang, X. J. Cui, Y. Q. Qi, X. D. Mu, X. L. Hou and Y. L. Zhu, *Green Chem.*, 2013, **15**, 2379.
- 34 J.-S. Lee, S.-I. Kim, J.-C. Yoon and J.-H. Jang, *ACS Nano* 2013, **7**, 6047.
- 35 Y. Zhu, S. Murali, M. D. Stoller, K. J. Ganesh, W. Cai, P. J. Ferreira, A. Pirkle, R. M. Wallace, K. A. Cychoz, M. Thommes, D. S. Su, E. A. Stach and R. S. Ruoff, *Science* 2011, **332**, 1537.
- 36 Z. Chen, W. Ren, L. Gao, B. Liu, S. Pei and H.-M. Cheng, *Nat. Mater.*, 2011, **10**, 424.
- 37 X.-H. Li, S. Kurasch, U. Kaiser and M. Antonietti, *Angew. Chem. Int. Ed.*, 2012, **51**, 9689.

- 38 Z. G. Xiong, L. L. Zhang and X. S. Zhao, *Chem.-Eur. J.*, 2011, **17**, 2428.
- 39 D. Margolese, J. A. Melero, S. C. Christiansen, B. F. Chmelka and G. D. Stucky, *Chem. Mater.*, 2000, **12**, 2448.
- 40 A. C. Ferrari and D. M. Basko, *Nat. Nanotechnol.*, 2013, **8**, 235.
- 41 A. C. Ferrari, J. C. Meyer, V. Scardaci, C. Casiraghi, M. Lazzeri, F. Mauri, S. Piscanec, D. Jiang, K. S. Novoselov, S. Roth and A. K. Geim, *Phys. Rev. Lett.*, 2006, **97**, 187401.
- 42 A. Zheng, S. J. Huang, S. B. Liu and F. Deng, *Phys. Chem. Chem. Phys.*, 2011, **13**, 14889.
- 43 Y. Chu, Z. Yu, A. Zheng, H. Fang, H. Zhang, S. J. Huang, S. B. Liu and F. Deng, *J. Phys. Chem. C* 2011, **115**, 7660.
- 44 M. D. Karra, K. J. Sutovich and K. T. Mueller, *J. Am. Chem. Soc.*, 2002, **124**, 902.
- 45 F. de Clippel, M. Dusselier, R. V. Rompaey, P. Vanelderen, J. Dijkmans, E. Makshina, L. Giebeler, S. Oswald, G. V. Baron, J. F. M. Denayer, P. P. Pescarmona, P. A. Jacobs and B. F. Sels, *J. Am. Chem. Soc.*, 2012, **134**, 10089.
- 46 T. Yokoi, H. Yoshitake, T. Yamada, Y. Kubota and T. Tatsumi, *J. Mater. Chem.*, 2006, **16**, 1125.

Table 1 The textural and acidic parameters of various catalysts.

Samples	Acid contents (mmol/g) ^a	N content (mmol/g) ^a	S _{BET} (m ² /g)	V _p ^b (cm ³ /g)	D _p (nm) ^c
GNC	-	1.82	945	3.1	3.8 & 33.7
GNC-[C ₃ N][SO ₃ CF ₃]	1.25	1.57	184	0.59	3.6 & 31.2
GNC-[C ₃ N][SO ₃ CF ₃] ^d	1.22	1.62	173	0.55	3.4 & 30.2
SBA-15-SO ₃ H	1.98	-	814	1.4	7.5
H ₃ PW ₁₂ O ₄₀ ^e	3.50	-	4.2	-	-
Amberlyst 15	4.30	-	45	0.31	40
[C ₃ vim][SO ₃ CF ₃] ^e	2.96	-	-	-	-
H ₂ SO ₄ ^e	10.20	-	-	-	-

^a The acid contents were measured by CHNS elemental analysis.

^b Pore volumes (V_p) were estimated at relative pressure p/p₀≈0.98.

^c Average pore diameters were estimated from BJH model.

^d GNC-[C₃N][SO₃CF₃] after being recycled for five times in transesterification of sunflower oil with methanol.

^e The acid contents of H₃PW₁₂O₄₀, [C₃vim][SO₃CF₃] and H₂SO₄ were calculated from molecular formula.

Table 2 Catalytic data in transesterification of sunflower oil with methanol over various samples ^a.

Catalysts	Conversion of esters (%)				
	Methyl palmitate (C _{16:0})	Methyl stearate (C _{18:0})	Methyl oleate (C _{18:1})	Methyl linoleate (C _{18:2})	Methyl heptacosane (C _{27:0})
	[C ₃ vim][SO ₃ CF ₃] ^b	89.1	94.8	95.2	93.1
H ₂ SO ₄ ^c	87.4	94.1	95.9	94.4	82.1
GNC-[C ₃ N][SO ₃ CF ₃]	88.5	93.6	94.7	92.3	81.4
GNC-[C ₃ N][SO ₃ CF ₃] ^d	84.3	89.1	92.3	90.7	78.3
H ₃ PW ₁₂ O ₄₀	58.9	59.2	54.3	60.1	50.9
Amberlyst 15	54.8	50.2	48.6	50.5	26.4
SBA-15-SO ₃ H	60.9	56.5	55.4	52.6	45.7

^a 1.0 g, sunflower oil; 2.47 mL, methanol; 0.15 g, catalyst; reaction temperature, 65 °C; reaction time, 18 h. The catalytic activity of the catalysts was characterized quantitatively by the conversion of fatty acid methyl esters (FAME, Y %) which was calculated as follows: Yield=(M_D/M_T)×100 %, where M_D and M_T are the number of moles of each FAME produced and expected, respectively. In this section, M_T is the number of moles of FAME catalyzed by 0.2 g of H₂SO₄ for 24 h, which was performed at 65 °C with the same content of feedstock as that of GNC-[C₃N][SO₃CF₃].

^b Imidazole based acidic ionic liquid synthesized by using the same procedure with

that of GNC-[C₃N][SO₃CF₃].

^c The same number of acidic sites as that of GNC-[C₃N][SO₃CF₃].

^d The 5th cycle in transesterification of sunflower oil with methanol.

Table 3 Yields of sugars and dehydration products in the depolymerization of Avicel catalyzed by various solid acids ^a.

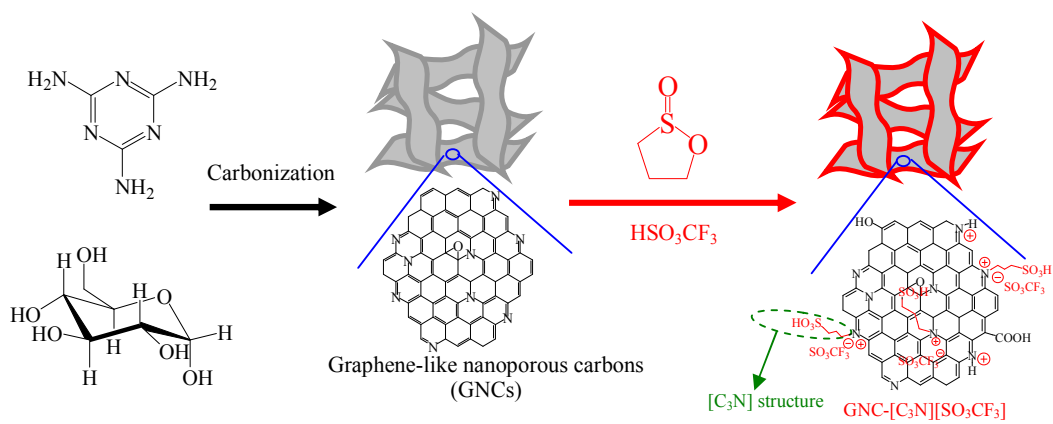
Run	Samples	Glucose yield (%) ^b	Cellobiose yield (%) ^b	HMF yield (%) ^b	TRS (%) ^c
1	Amberlyst 15 ^c	14.3	17.5	3.2	40.5
2	HCl ^d	39.8	20.4	10.7	87.1
3	[C ₃ vim][SO ₃ CF ₃] ^d	26.3	34.5	10.1	84.9
4	GNC-[C ₃ N][SO ₃ CF ₃]	44.1	32.7	11.6	94.6

^a 0.1 g, Avicel; 1.5 g, [C₄mim]Cl ionic liquid, and 0.5 mL, DMSO mixed solvents; 20 mg, catalyst; reaction temperature, 100 °C; reaction time, 5 h.

^b Measured by HPLC method.

^c Measured by DNS method.

^d The same number of acidic sites as in GNC-[C₃N][SO₃CF₃].



Scheme 1 The procedures for synthesizing GNC-[C₃N][SO₃CF₃].

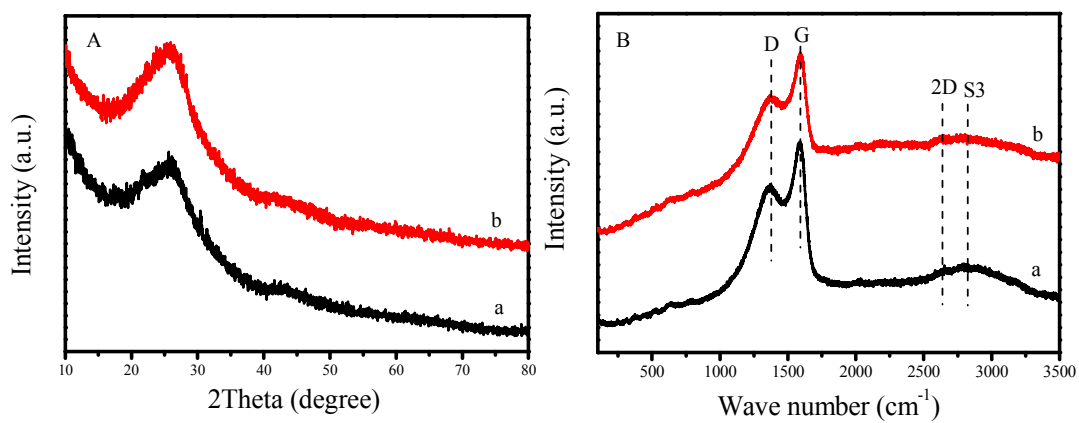


Figure 1 (A) XRD patterns and (B) Raman spectra of (a) GNC and (b) GNC-[C₃N][SO₃CF₃].

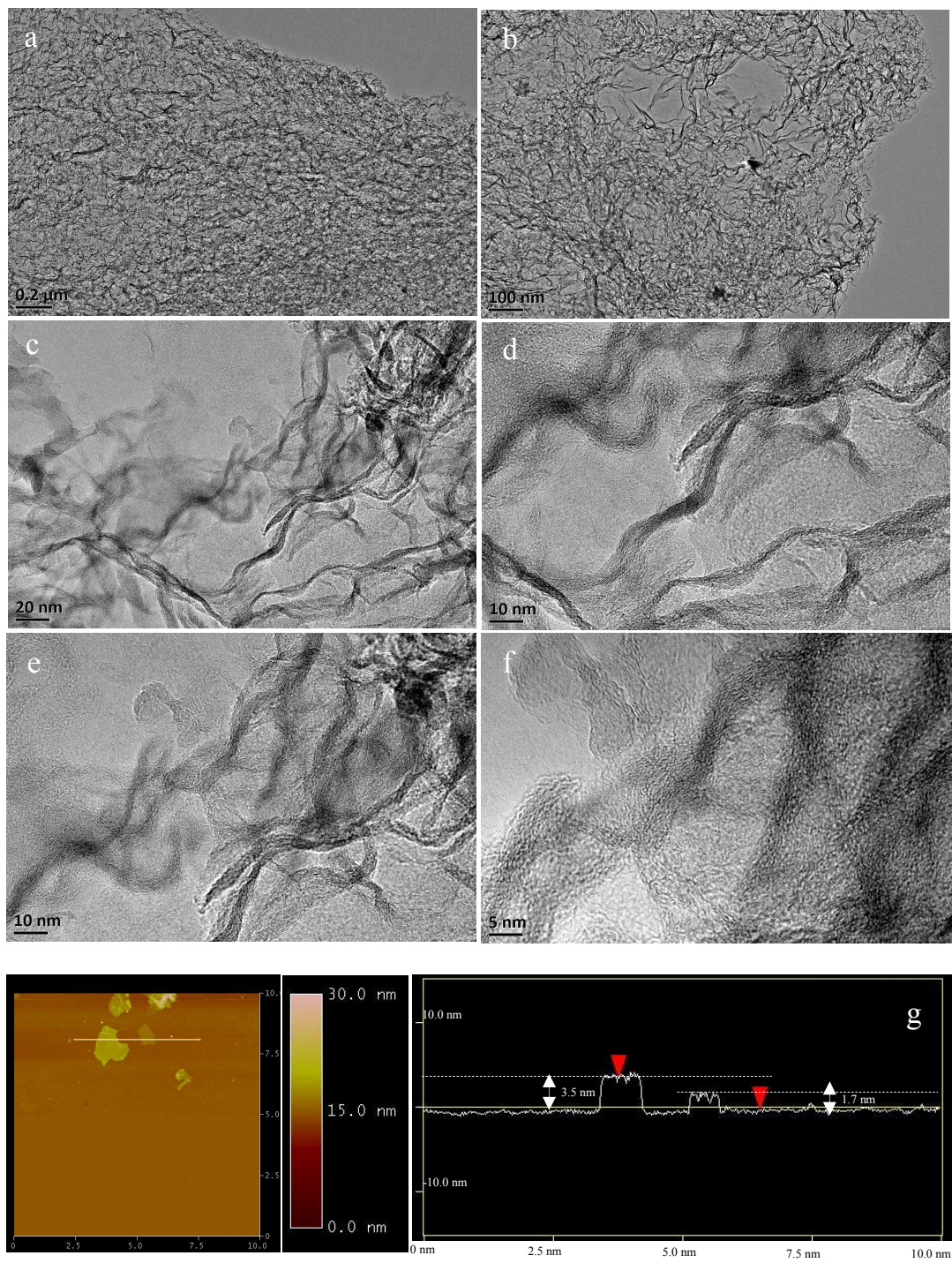


Figure 2 (a, b) TEM images, (c-f) high-resolved TEM images, and (g) AFM image and corresponding thickness analysis of GNC-[C₃N][SO₃CF₃].

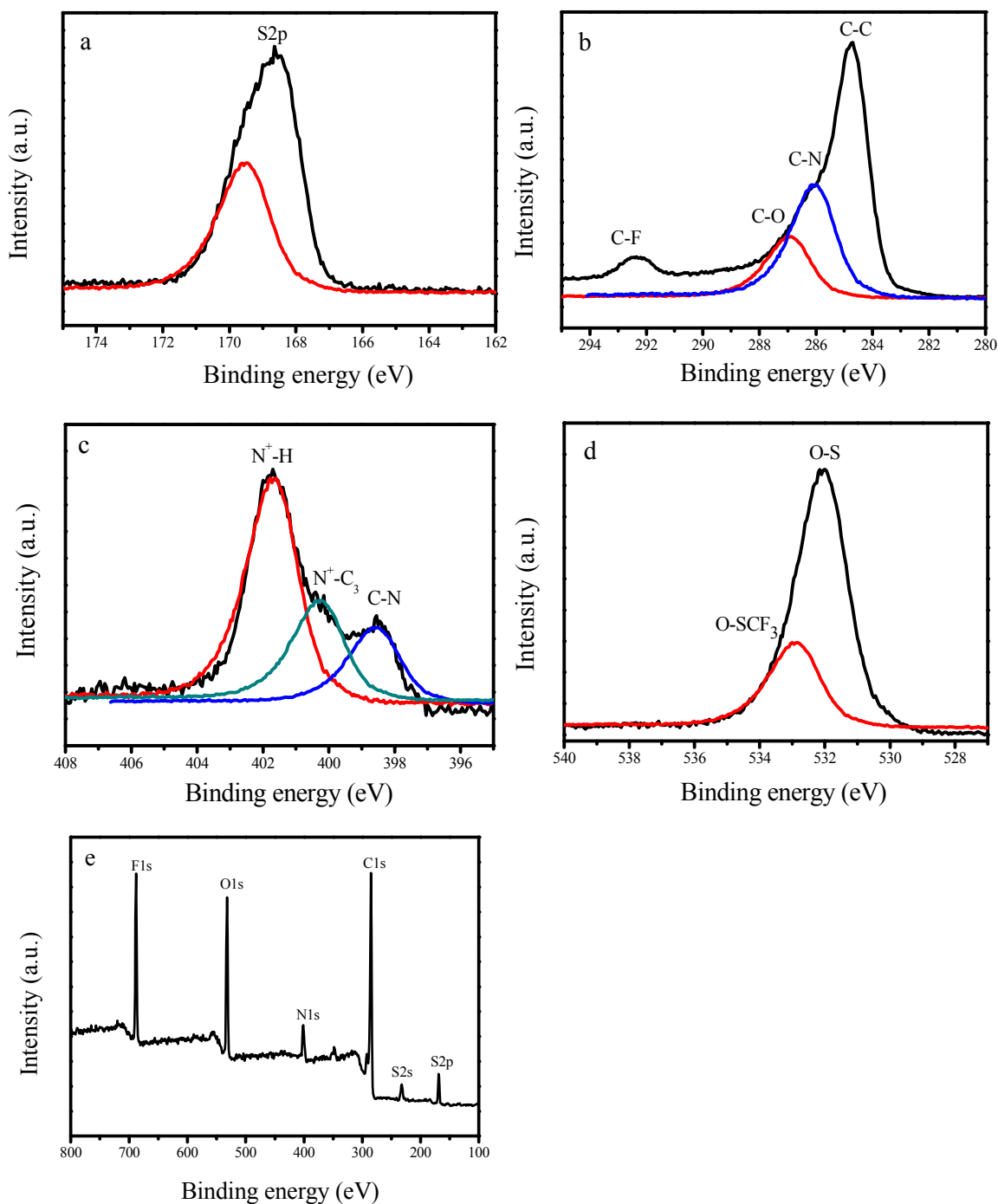


Figure 3 XPS spectra of (a) S_{2p}, (b) C_{1s}, (c) N_{1s}, (d) O_{1s} and (e) survey of GNC-[C₃N][SO₃CF₃].

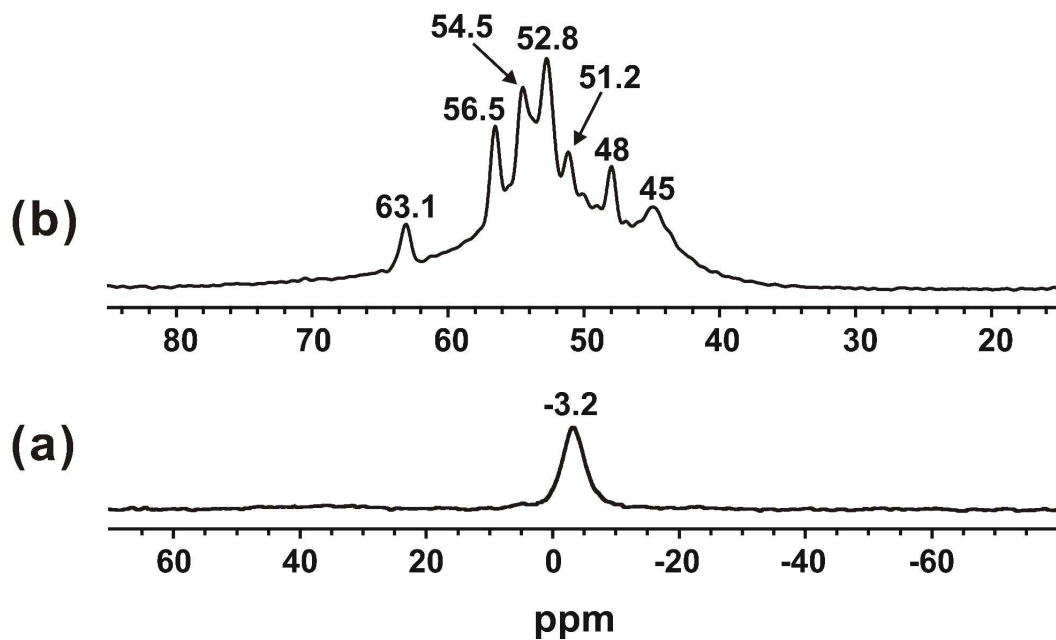


Figure 4 Room temperature ^{31}P MAS NMR spectra of adsorbed (a) TMP acquired with proton decoupling, and (b) TMPO of GNC-[C₃N][SO₃CF₃].

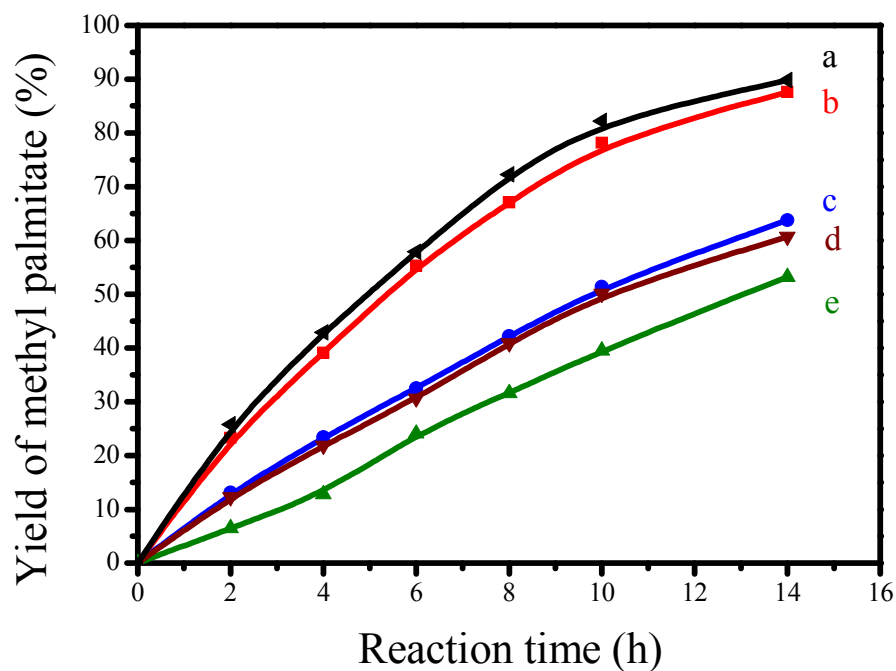


Figure 5 Dependences of catalytic activities on the time in transesterification of tripalmitin with methanol catalyzed by (a) $[C_3vim][SO_3CF_3]$ (the same number of acidic sites as that of $GNC-[C_3N][SO_3CF_3]$), (b) $GNC-[C_3N][SO_3CF_3]$, (c) $H_3PW_{12}O_{40}$, (d) $SBA-15-SO_3H$ and (e) Amberlyst 15.

Reaction condition: 0.84 g, tripalmitin; 2.47 mL, methanol; 0.1 g, catalyst; reaction temperature, 65 °C; reaction time, 14 h.

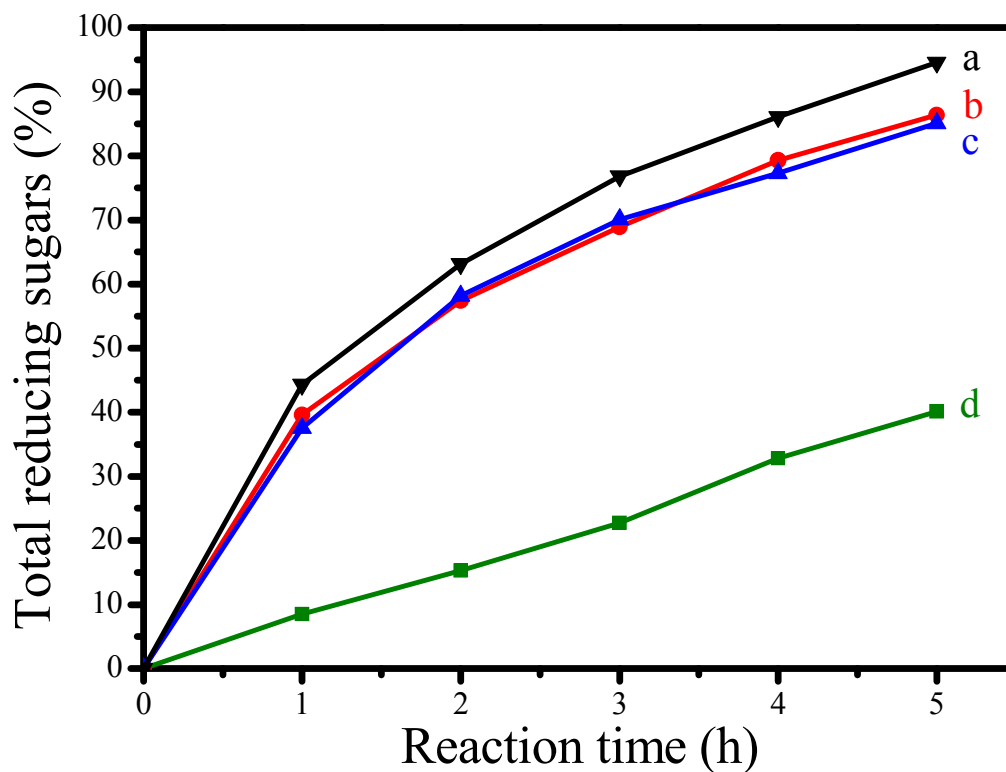
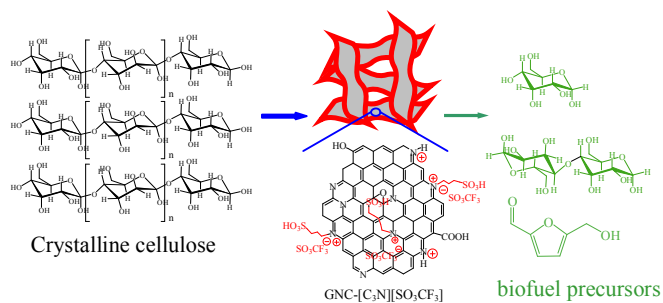


Figure 6 Dependences of catalytic activities on the time in depolymerization of Avicel into sugars catalyzed by (a) GNC-[C₃N][SO₃CF₃], (b) HCl, (c) [C₃vim][SO₃CF₃] and (d) Amberlyst 15 (b, c, d was used the same number of acidic sites as in GNC-[C₃N][SO₃CF₃]).

Reaction condition: 0.1 g, Avicel; 1.5 g, [C₄mim]Cl ionic liquid, and 0.5 mL, DMSO mixed solvents; 20 mg, catalyst; reaction temperature, 100 °C; reaction time, 5 h. The total reducing sugars were monitored by 3,5-dinitrosalicylic acid (DNS) reagent.

Graphical abstract



Strong acid ionic liquids and sulfonic groups bifunctional graphene-like nanoporous carbon with abundant nanopores, controlled acidity and excellent catalytic activity for biomass transformation have been successfully prepared in this work.